UNIVERSITY POLITEHNICA BUCHAREST

FACULTY OF AEROSPACE ENGINEERING

Design and build of aircraft models at a favorable scale in order to check the similitude requirements that leads to aircraft design coefficients.

PhD - Summary

PROF. COORD.: Prof. Dr. Ing. Stelian Găletușe

PhD: Ing. Anton Ștefan Mihai

BUCHAREST 2019

Contents

1 Context and Objectives

In recent years there has been an exponential increase in the UAVs domain, which has been fueled by both the military and civilian area. In the civil area the UAV can be used for aerial surveillance and photogrammetry. Practically, the payload can include any type of sensor that provides data in the field of interest, the UAV is considered a platform that performs the role of carrying the sensor by air. Since the sensor mounted in the payload can be of different sizes and masses, usually, the producing companies do not limit themselves to just one UAV, they are developing a whole series of UAVs ranging from micro area (0,5 - 1 kg) up to UAVs as large as passenger transport airplanes. Depending on the class in which the UAV is located, the producer company must comply with certain restrictions when generating a new product which means we have new design criteria to be considered.

Thus, starting from private needs, the doctoral thesis aims to estimate the dynamic characteristics of an UAV, starting from an UAV already made and ready to fly but which is at a different scale. Estimating the dynamic characteristics, or better said the similarities between two UAVs at different scales, helps us to use the same automatic pilot adjustments with reference to the settings of PID parameters on the first flight.

The purpose of flight tests is to validate aerodynamic characteristics or provide predictions where the theory is deficient. For reasons of material costs, when designing a new aircraft, it is originally constructed at a lower scale in order to validate preliminary theoretical calculations.

It is highly known that, in order to validate flight tests or to extrapolate the results to the 1:1-scale plane, certain similitude criteria must be met. In addition to the geometric similarity and the angle of attack, the Reynolds and Froude criteria must be met. Because we are dealing with subsonic and incompressible flight (surveillance UAVs) Mach number will not be taken into account. There are also other similitude parameters which may have a major influence in certain situations or if the aeroelastic effect is considered. In general, you can't fulfill all the similitude requirements when a flight test is performed. Most of the flight tests are programmed to fulfill only one or a few similitude requirements, one of the major factors in flight test is how much the similitude requirements were fulfilled.

The doctoral thesis is focused around the flying wing UAV manufactured and designed at AFT Design company. At this moment there are operational only UAV Hirrus (2 wing sets; different wingspan, aspect ratio and sweep in order to have the same weight center) and UAV Muros, two flying wings with geometric similitude. The goal is to extrapolate the results towards a UAV of 2 or 4 times larger.

First step is about developing a dynamic model using Etkin as a main reference and after that we will apply this model on the same geometry but at a different scale. The dynamic model, along with the stability matrix **A** and the control matrix **B** also contains the step response at 1-degree flap deflection. The last part is about comparing the theoretical plane polar with the experimental results obtained from gliding flight.

Starting from Etkin dynamic model with additions from Nelson, Cook and Platfus the following parameters resulted for the dynamic model:

- f_s, scale factor - parameter that multiplies any geometrical size, it supplies the geometric characteristics of the next UAV;
- p_1, mass ratio - parameter that multiplies the mass of the same UAV;
- p_2, moment of inertia ratio - parameter that is taking into account the mass distribution inside UAV.

The inertia moments have been theoretically determined by the 3D design software SolidWorks; each major component was taken into account depending on its complexity. Having a certain mass, you can't alter too much inertia moment distribution inside UAV so depending on inertia moment value there is a limit until you'll be able to make the flight test.

Mathematically we have to solve a nonlinear sister of equations with the following inputs: Damping ratio of the full-scale UAV must be equal to the damping ratio of the scale model and the same situation is considered for undamped natural frequency.

2 UAV Flying Wing

The plane to which we refer is part of the Hirrus UAVs family, produced by the AFT Design company, more specifically is the 15 kg maximum take-off mass version. An important element of the geometry is that the wing is not exactly distinguished from the fuselage, the UAV having the loft between the wing and the fuselage quite generously. In the figure Fig. 2.1. the general geometry of the plane is outlined. This version will be taken as a reference, the plane is already ready to fly.

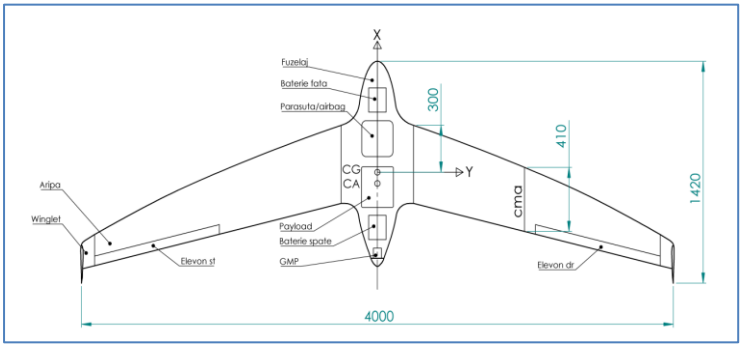

Fig. 2.1. View from above UAV-BWB

2.1 Aerodynamic properties

The aerodynamic coefficients for this model are expressed in the reference system of the plane illustrated in Fig. 2.1. These coefficients are generally based on angular speeds (p, q, r), flight incidence and side-slip angle (α, β), geometry changes meaning elevon deflection (δe) and positioning of the gravity center; in our case we have only one value, 300 mm referenced from the front of wing embed with the fuselage.

The longitudinal and lateral movement equations, linearized and decoupled are shown in Fig. 2.2 and Fig. 2.3

$$\begin{bmatrix} \Delta\dot{u} \\ \dot{w} \\ \dot{q} \\ \Delta\dot{\theta} \end{bmatrix} = \begin{bmatrix} \frac{X_u}{m} & \frac{X_w}{m} & 0 & -g\cdot cos\theta \\ \frac{Z_u}{m - Z_{\dot{w}}} & \frac{Z_w}{m - Z_{\dot{w}}} & \frac{Z_q + m\cdot u_0}{m - Z_{\dot{w}}} & \frac{-m\cdot g\cdot sin\theta}{m - Z_{\dot{w}}} \\ \frac{1}{I_y}\left[M_u + \frac{M_{\dot{w}} Z_u}{m - Z_{\dot{w}}}\right] & \frac{1}{I_y}\left[M_w + \frac{M_{\dot{w}} Z_w}{m - Z_{\dot{w}}}\right] & \frac{1}{I_y}\left[M_q + \frac{M_{\dot{w}}(Z_w + m\cdot u_0)}{m - Z_{\dot{w}}}\right] & \frac{-M_{\dot{w}} mgsin\theta}{I_y(m - Z_{\dot{w}})} \\ 0 & 0 & 1 & 0 \end{bmatrix} \cdot \begin{bmatrix} \Delta u \\ w \\ q \\ \theta \end{bmatrix} + \begin{bmatrix} \frac{\Delta X_c}{m} \\ \frac{\Delta Z_c}{m - Z_{\dot{w}}} \\ \frac{\Delta M_c}{I_y} + \frac{M_{\dot{w}}}{I_y}\frac{\Delta Z_c}{m - Z_{\dot{w}}} \\ 0 \end{bmatrix}$$

Fig. 2.2 Motion equations on the longitudinal channel, Etkin [1]

$$\begin{bmatrix} \dot{v} \\ \dot{p} \\ \dot{r} \\ \dot{\varphi} \end{bmatrix} = \begin{bmatrix} \frac{Y_v}{m} & \frac{Y_p}{m} & \frac{Y_r}{m} - u_0 & g \cdot cos\theta \\ \frac{L_v}{I'_x} + I'_{zx}N_v & \frac{L_p}{I'_x} + I'_{zx}N_p & \frac{L_r}{I'_x} + I'_{zx}N_r & 0 \\ I'_{zx}L_v + \frac{N_v}{I'_z} & I'_{zx}L_p + \frac{N_p}{I'_z} & I'_{zx}L_r + \frac{N_r}{I'_z} & 0 \\ 0 & 0 & tan\theta & 0 \end{bmatrix} \cdot \begin{bmatrix} v \\ p \\ r \\ \varphi \end{bmatrix} + \begin{bmatrix} \frac{\Delta Y_c}{m} \\ \frac{\Delta L_c}{I'_x} + I'_{zx}N_c \\ I'_{zx}\Delta L_c + \frac{\Delta N_c}{I'_z} \\ 0 \end{bmatrix}$$

$$I'_x = \frac{(I_x I_z - I_{zx}^2)}{I_z}; I'_z = \frac{(I_x I_z - I_{zx}^2)}{I_x}; \; I'_{zx} = \frac{I_{zx}}{(I_x I_z - I_{xz}^2)}$$

Fig. 2.3. Lateral-directional Motion equations, Etkin [1]

Each of the forces and moments used in the above equations can be obtained by their partial derivation according to the illustrated variables. However, because we apply our relationships on a flying wing, we can express the force coefficient after the X-axis, Cx, depending on the Z-axis force coefficient, Cz.

2.2 Dynamic airplane stability

2.2.1 Input data for reference movement

For the aerodynamic study it is considered the reference movement (horizontal unaccelerated rectilinear flight, elevon as an elevator of -6 degrees) characterized by the values of the parameters from Table 2.1.

Table 2.1. Reference Movement

Parameter	Symbol	Value	U.M.
Wing area	S	1.569	m^2
Wing-span	b	4	m
Average aerodynamic chord	Cma	0.41	m
Mass	m	10.517	kg
Flight Speed (TAS)	u_0	18	m/s
Air density	ρ	1.225	Kg/m^3
Values for reference movement (at equilibrium)			
Angle of incident	α	3.2	grade
Lateral sliding angle	β	0	grade
Elevon deflection (aileron)	δ_a	0	grade
Elevon deflection (elevator)	δ_e	-6	grade
Lift coefficient	Cz	0.329567	-
Drag coefficient	Cx	0.014142	-
Lateral force coefficient	Cy	0	-

2.2.2 Longitudinal dynamics

Longitudinal dynamic can be written as a linear system (1):

$$\boldsymbol{E} \cdot \dot{\boldsymbol{X}} = \boldsymbol{A} \cdot \boldsymbol{X} + \boldsymbol{B} \cdot \delta e \tag{1}$$

In the equation (1), because the derivatives $X_{\dot{w}}, Z_{\dot{w}}, M_{\dot{w}}, M_{\theta}$ are considered null, the matrix **E** becomes unity matrix. The influence of flight altitude has been neglected (air density variation with altitude) for longitudinal dynamics because the influence is negligible. The eigenvalues of the stability matrix shall be determined in MATLAB

with command eig(**A**), the following results were obtained: $eig(\boldsymbol{A}) = (-4.01795 \pm 6{,}86701i;\ -0.033906 \pm 0.758788i)$. The system is stable if the eigenvalues have the real part negative.

The stability matrix **A**:

$$\boldsymbol{A} = \begin{bmatrix} \frac{X_u}{m_{av}} & \frac{Z_u}{m_{av}-Z_{wp}} & 0 & -g\cdot\cos(\theta_0) \\ \frac{X_w}{m_{av}} & \frac{Z_w}{m_{av}-Z_{wp}} & \frac{Z_q+m_{av}u_0}{m_{av}-Z_{\dot{w}}} & \frac{-m_{av}\cdot g\cdot\sin(\theta_0)}{m_{av}-Z_{\dot{w}}} \\ \frac{1}{I_y}\left[M_u+\frac{M_{\dot{w}}Z_u}{m_{av}-Z_{\dot{w}}}\right] & \frac{1}{I_y}\left[M_w+\frac{M_{\dot{w}}Z_w}{m_{av}-Z_{\dot{w}}}\right] & \frac{1}{I_y}\left[M_q+\frac{M_{\dot{w}}(Z_q+m_{av}u_0)}{m_{av}-Z_{\dot{w}}}\right] & \frac{M_{\dot{w}}m_{av}\cdot g\cdot\sin(\theta_0)}{I_y(m_{av}-Z_{\dot{w}})} \\ 0 & 0 & 1 & 0 \end{bmatrix} \quad (2)$$

$$= \begin{bmatrix} -0{,}07013 & 0{,}2720530 & 0 & -9{,}80665 \\ 0{,}722399 & -6{,}575451 & 16{,}185610 & 0 \\ 0{,}932816 & -3{,}427576 & -1{,}546253 & 0 \\ 0 & 0 & 1 & 0 \end{bmatrix}$$

Control matrix **B**:

$$\boldsymbol{B} = \begin{bmatrix} \frac{X_{\delta e}}{m} & \frac{X_{\delta p}}{m} \\ \frac{Z_{\delta e}}{m_{av}-Z_{wp}} & \frac{Z_{\delta p}}{m_{av}-Z_{wp}} \\ \frac{M_{\delta e}}{I_y}+\frac{M_{wp}Z_{\delta e}}{I_y(m_{av}-Z_{wp})} & \frac{M_{\delta p}}{I_y}+\frac{M_{wp}Z_{\delta p}}{I_y(m_{av}-Z_{wp})} \\ 0 & 0 \end{bmatrix} = \begin{bmatrix} 0 & 0 \\ -19{,}964423 & 0 \\ -49{,}645287 & 0 \\ 0 & 0 \end{bmatrix} \quad (3)$$

Routh stability criteria

The matrix determinant is calculated from $|\boldsymbol{A} - \boldsymbol{I}\lambda|$ and a 4th grade polynomial equation (λ) is obtained $A\lambda^4 + B\lambda^3 + C\lambda^2 + D\lambda + E$. According to the Routh stability criteria we do not have an unstable result if E and R are greater than 0; R is obtained from the relation $R = D(BC - AD) - B^2E = 2557{,}13$. Looking at the values obtained we can conclude that we don't have unstable modes.

Transfer functions, longitudinal channel

The transfer functions on the longitudinal channel G(s) are obtained by applying the Laplace transformation to the equation $\dot{\boldsymbol{x}} = \boldsymbol{Ax} + \boldsymbol{Bc}$.

$$\Delta_u(s) = \begin{vmatrix} B_{0,0} & A_{0,1} & A_{0,2} & A_{0,3} \\ B_{1,0} & A_{1,1} - s & A_{1,2} & A_{1,3} \\ B_{2,0} & A_{2,1} & A_{2,2} - s & A_{2,3} \\ B_{3,0} & A_{3,1} & A_{3,2} & A_{3,3} - s \end{vmatrix} \rightarrow$$

$$\rightarrow 5{,}43138944 \cdot s^2 - 259{,}85005113 \cdot s - 2530{,}21939750$$

$$\Delta_w(s) = \begin{vmatrix} A_{0,0} - s & B_{0,0} & A_{0,2} & A_{0,3} \\ A_{1,0} & B_{1,0} & A_{1,2} & A_{1,3} \\ A_{2,0} & B_{2,0} & A_{2,2} - s & A_{2,3} \\ A_{3,0} & B_{3,0} & A_{3,2} & A_{3,3} - s \end{vmatrix} \rightarrow$$

$$\rightarrow 19{,}96442274 \cdot s^3 + 835{,}80952663 \cdot s^2 + 58{,}52247097 \cdot s - 169{,}07214419$$

$$\Delta_q(s) = \begin{vmatrix} A_{0,0} - s & A_{0,1} & B_{0,0} & A_{0,3} \\ A_{1,0} & A_{1,1} - s & B_{1,0} & A_{1,3} \\ A_{2,0} & A_{2,1} & B_{2,0} & A_{2,3} \\ A_{3,0} & A_{3,1} & B_{3,0} & A_{3,3} - s \end{vmatrix} \rightarrow$$

$$\rightarrow 49{,}64528678 \cdot s^3 + 261{,}49251631 \cdot s^2 + 13{,}40558154 \cdot s$$

$$\Delta_\theta(s) = \begin{vmatrix} A_{0,0} - s & A_{0,1} & A_{0,2} & B_{0,0} \\ A_{1,0} & A_{1,1} - s & A_{1,2} & B_{1,0} \\ A_{2,0} & A_{2,1} & A_{2,2} - s & B_{2,0} \\ A_{3,0} & A_{3,1} & A_{3,2} & B_{3,0} \end{vmatrix} \rightarrow$$

$$\rightarrow 49{,}64528678 \cdot s^3 + 261{,}49251631 \cdot s^2 + 13{,}40558154 \cdot s$$

$$\Delta(s) = |\boldsymbol{A} - \boldsymbol{I} \cdot \lambda| =$$

$$= s^4 + 8{,}19184072 \cdot s^3 + 66{,}01781558 \cdot s^2 + 9{,}34048478 \cdot s + 2530{,}21939750$$

$$\begin{aligned} G_{u\delta e} &= -\frac{\Delta u(s)}{\Delta(s)} \\ G_{w\delta e} &= -\frac{\Delta w(s)}{\Delta(s)} \\ G_{q\delta e} &= -\frac{\Delta q(s)}{\Delta(s)} \\ G_{\theta\delta e} &= -\frac{\Delta \theta(s)}{\Delta(s)} \end{aligned} \tag{4}$$

In order to illustrate the time response of the system (t = 0:100) at a 1-degree elevator deflection ($\delta e = 1\text{deg}$), the reversed Laplace transform is calculated and the time evolution of disturbances can be found in (5).

$$\begin{aligned} u(t) &= invLaplace(G_{u\delta e}) \cdot \delta e \\ w(t) &= invLaplace(G_{w\delta e}) \cdot \delta e \\ q(t) &= invLaplace(G_{q\delta e}) \cdot \delta e \\ \theta(t) &= invLaplace(G_{\theta\delta e}) \cdot \delta e \end{aligned} \tag{5}$$

2.2.3 Lateral-directional dynamics

The lateral-directional dynamics of an airplane can be written (6):

$$\dot{\boldsymbol{X}} = \boldsymbol{A} \cdot \boldsymbol{X} + \boldsymbol{B} \cdot \boldsymbol{C} \tag{6}$$

where matrix **C** is the command matrix, in our case we have only elevons (ailerons). The matrix **A** is represented by the formulas:

$$\boldsymbol{A} = \begin{bmatrix} \frac{Y_v}{m_{av}} & \frac{Y_p}{m_{av}} & \frac{Y_r}{m_{av}} - u_0 & g\cos(\theta_0) \\ \frac{L_v}{I_x^`} + I_{zx}^` N_v & \frac{L_p}{I_x^`} + I_{zx}^` N_p & \frac{L_r}{I_x^`} + I_{zx}^` N_r & 0 \\ I_{zx}^` L_v + \frac{N_v}{I_z^`} & I_{zx}^` L_p + \frac{N_p}{I_z^`} & I_{zx}^` L_r + \frac{N_r}{I_z^`} & 0 \\ 0 & 1 & \tan(\theta_0) & 0 \end{bmatrix}$$

$$= \begin{bmatrix} -0{,}237 & -0{,}0261 & -17{,}9 & 9{,}81 \\ -0{,}0669 & 0 & 0{,}0296 & 0 \\ 0{,}204 & 0{,}0224 & -0{,}0904 & 0 \\ 0 & 1 & 0 & 0 \end{bmatrix}$$

and matrix **B**,$\boldsymbol{B} = \begin{bmatrix} \frac{Y_{\delta a}}{m_{av}} \\ \frac{L_{\delta a}}{I_x^`} + I_{zx}^` N_{\delta a} \\ I_{zx}^` L_{\delta a} + \frac{N_{\delta a}}{I_z^`} \\ 0 \end{bmatrix} = \begin{bmatrix} 0 \\ 29{,}730626 \\ 1{,}155358 \\ 0 \end{bmatrix}$

The eigenvalues of the stability matrix **A** are: $eig(\boldsymbol{A}) = [-0{,}077349 \pm 1{,}907326i \mid -0{,}172556 \mid -0{,}0001460334]$

where:

$\lambda 1 = -0{,}0001460334$; Spiral mode

$\lambda 2 = -0{,}172556$; Rolling mode

$\lambda 3 = -0{,}077349 \pm 1{,}907326i$; Side oscillation mode or Dutch roll

Routh stability criteria:

The matrix determinant is calculated from $|\boldsymbol{A} - \boldsymbol{I}\lambda|$ and a 4th grade polynomial equation (λ) is obtained, $A\lambda^4 + B\lambda^3 + C\lambda^2 + D\lambda + E$. According to the Routh stability criteria we do not have an unstable result if E and R are greater than 0; R is obtained from the relation $R = D(BC - AD) - B^2E = 0{,}360239$. Looking at the values obtained we can conclude that we don't have unstable modes.

Transfer functions, lateral-directional channel

$$\Delta_v(s) = \begin{vmatrix} B_{0,0} & A_{0,1} & A_{0,2} & A_{0,3} \\ B_{1,0} & A_{1,1} - s & A_{1,2} & A_{1,3} \\ B_{2,0} & A_{2,1} & A_{2,2} - s & A_{2,3} \\ B_{3,0} & A_{3,1} & A_{3,2} & A_{3,3} - s \end{vmatrix} \rightarrow$$

$$\rightarrow 21{,}450664 \cdot s^2 - 279{,}547332 \cdot s - 26{,}681181$$

$$\Delta_p(s) = \begin{vmatrix} A_{0,0} - s & B_{0,0} & A_{0,2} & A_{0,3} \\ A_{1,0} & B_{1,0} & A_{1,2} & A_{1,3} \\ A_{2,0} & B_{2,0} & A_{2,2} - s & A_{2,3} \\ A_{3,0} & B_{3,0} & A_{3,2} & A_{3,3} - s \end{vmatrix} \rightarrow$$

$$\rightarrow -29{,}730626 \cdot s^3 - 9{,}774926 \cdot s^2 = 110{,}569858 \cdot s$$

$$\Delta_r(s) = \begin{vmatrix} A_{0,0} - s & A_{0,1} & B_{0,0} & A_{0,3} \\ A_{1,0} & A_{1,1} - s & B_{1,0} & A_{1,3} \\ A_{2,0} & A_{2,1} & B_{2,0} & A_{2,3} \\ A_{3,0} & A_{3,1} & B_{3,0} & A_{3,3} - s \end{vmatrix} \rightarrow$$

$$\rightarrow -29{,}730626 \cdot s^3 \pm 7{,}721414 \cdot s^2 + 0{,}051922 \cdot s - 78{,}991921$$

$$\Delta_\phi(s) = \begin{vmatrix} A_{0,0} - s & A_{0,1} & A_{0,2} & B_{0,0} \\ A_{1,0} & A_{1,1} - s & A_{1,2} & B_{1,0} \\ A_{2,0} & A_{2,1} & A_{2,2} - s & B_{2,0} \\ A_{3,0} & A_{3,1} & A_{3,2} & B_{3,0} \end{vmatrix} \rightarrow$$

$$\rightarrow -29{,}730626 \cdot s^2 - 10{,}621794 \cdot s - 144{,}986485$$

$$\Delta(s) = |\boldsymbol{A} - \boldsymbol{I} \cdot s| =$$

$$= s^4 + 0{,}327631 \cdot s^3 + 3{,}669839 \cdot s^2 + 0{,}629165 \cdot s + 2{,}186745$$

$$\begin{aligned} G_{v\delta a} &= -\frac{\Delta_v(s)}{\Delta(s)} \\ G_{p\delta a} &= -\frac{\Delta_p(s)}{\Delta(s)} \\ G_{r\delta a} &= -\frac{\Delta_r(s)}{\Delta(s)} \end{aligned} \qquad (7)$$

$$G_{\phi\delta a} = -\frac{\Delta\phi(s)}{\Delta(s)}$$

Similar to the longitudinal channel, in order to calculate the time response of the system (t= 0:50) at 1-degree aileron deflection ($\delta a = 1\text{deg}$) the reversed Laplace transform is used.

$$\begin{aligned} v(t) &= invLaplace(G_{v\delta a}) \cdot \delta a \\ p(t) &= invLaplace(G_{p\delta a}) \cdot \delta a \\ r(t) &= invLaplace(G_{r\delta a}) \cdot \delta a \\ \phi(t) &= invLaplace(G_{\phi\delta a}) \cdot \delta a \end{aligned} \tag{8}$$

Following the aerodynamic calculations resulted that the UAV is stable on both longitudinal and lateral-directional channel, following a disturbance of 1 degree of elevon deflection the parameters of the system return to its original state. The reference movement was considered the one with the elevon as an elevator at -6 degrees deflection.

3 Similitude criteria used for scaling

The required similitude criteria are presented in the reference, they were used to generate various points of calculation and relations between f_s, p_1 and p_2.

Plane scaling involves geometric scaling in all aspects including the gaps between the command surfaces. In any case, the similarity of the Reynolds number must be fulfilled in order to have

the same transition point on the airfoil, the thickness of the boundary layer and possible interference by the interaction of the Reynolds number with Mach number (compressibility effects). In this case, I have expressed the variation of stability derivatives with the Reynolds number or better said the variation of the stability derivatives (those that are related to CD - drag) with the model scale. It's also necessary for the scaling that the angle of attack, the lateral side-slip angle, the position of the control surface to be the same, which leads to a convenient choice for the reference movement (horizontal, rectilinear flight and unaccelerated).

3.1 Relative density factor

As shown in the reference, the relative density factor, $\frac{m}{\rho l^3}$ is a basic similitude parameter in the aerodynamic forces. This factor is important in studying the phenomenon of flutter but also in studying the characteristics of stability and control.

The relative moment of inertia, $\frac{I}{\rho l^5}$ has the same significance for the equations of the moment as the relative density factor has it for the equations of the forces. Starting from (9)

$$I_y \dot{q} = C_m 1/2 \rho V^2 Sc \qquad (9)$$

in dimensional format it follows:

$$C_m = 2\left(\frac{I_y}{\rho S c}\right)\left(\frac{\dot{q}}{V^2}\right) = 2\left(\frac{I_y}{\rho S c^3}\right)\left(\frac{\dot{q}c^2}{V^2}\right) = f\left(\frac{I_y}{\rho l^5}, \frac{\dot{\Omega} l^2}{V^2}\right)$$

$$C_m = f\left[\frac{m}{\rho l^3}, \left(\frac{k}{l}\right)^2, \frac{\dot{\Omega} l^2}{V^2}\right] \qquad (10)$$

For the scale model to have the same moment coefficient as the 1:1 scale plane, the relative moment of inertia, $\frac{I}{\rho l^5}$, the reduced angular acceleration, $\frac{\dot{\Omega} l^2}{V^2}$, must be identical. For a rigid airplane, the moment of inertia can be adjusted by redistributing the masses inside the airplane in order to have the same K/L ratio, assuming that the relative density factor is already met.

In this case, this criterion provides us with a relation between UAV scale (parameter fs) and the UAV mass (parameter p_1). For example, for a scale factor of 2, to comply with the relative density criteria, we will obtain a value for p_2 of 8. This relation is added to the MATLAB equation system, it remains to be seen how it varies (mass distribution) to solve the system of equations p_2.

$\frac{m_1}{\rho l_1^3} = \frac{m_2}{\rho l_2^3}$, where $m_2 = m_1 \cdot p1,\ l_2 = l_1 \cdot fs$

Thus, we have a relation between us fs and p_1:

$$\frac{m_1}{\rho l_1^3} = \frac{m_2}{\rho l_2^3} <=> \frac{m_1}{l_1^3} = \frac{m_1 \cdot p1}{(l_1 \cdot fs)^3} <=> p1 = fs^3 \qquad (11)$$

From this relation (11) it actually results a method for scaling the UAVs by fulfilling the relative density factor criteria.

4 Short-period mode approximation, parameterized system

Taking into account the form of stability derivatives previously presented the stability matrix **A** will result as a function of f_s, $p_1$and p_2.

On the longitudinal channel, considering the short-period mode approximation:

$$\begin{bmatrix}\dot{w}\\ \dot{q}\end{bmatrix}=\begin{bmatrix}\frac{Z_w}{m_{av}} & u_0\\ \frac{1}{I_y}\left(M_w+\frac{M_{\dot{w}}Z_w}{m_{av}}\right) & \frac{1}{I_y}(M_q+M_{\dot{w}}u_0)\end{bmatrix}\cdot\begin{bmatrix}w\\ q\end{bmatrix} \qquad (12)$$

$$\left(\frac{Z_w}{m_{av}}-\lambda\right)\cdot\left(\frac{M_q}{I_y}+\frac{M_{\dot{w}}u_0}{I_y}-\lambda\right)-\frac{1}{I_y}\left(M_w+\frac{M_{\dot{w}}Z_w}{m_{av}}\right)u_0=0$$

$$\frac{Z_w}{m_{av}}\frac{M_q}{I_y}+\frac{Z_w}{m_{av}}\frac{M_{\dot{w}}u_0}{I_y}-\frac{Z_w}{m_{av}}\lambda-\lambda\frac{M_q}{I_y}-\lambda\frac{M_{\dot{w}}u_0}{I_y}+\lambda^2-\frac{M_wu_0}{I_y}-\frac{M_{\dot{w}}Z_wu_0}{m_{av}I_y}=$$

$$\lambda^2-\lambda\left(\frac{Z_\alpha}{m_{av}u_0}+\frac{M_q}{I_y}+\frac{M_{\dot{\alpha}}}{I_y}\right)+\left(\frac{Z_\alpha}{m_{av}u_0}\frac{M_q}{I_y}-\frac{M_\alpha}{I_y}\right)=0 \qquad (13)$$

the following relations are obtained for the damping factor ζ_{sp} and the undamped natural frequency ω_{nsp} .

$$\zeta_{sp} = \frac{\frac{Z_\alpha}{m_{av}u_0} + \frac{M_q}{I_y} + \frac{M_{\dot{\alpha}}}{I_y}}{2 \cdot \omega_{nsp}} = -\frac{\lambda_1 + \lambda_2}{2 \cdot \omega_{nsp}} = \zeta_{dat} \tag{14}$$

$$\omega_{nsp} = \sqrt{\frac{Z_\alpha}{m_{av}u_0}\frac{M_q}{I_y} - \frac{M_\alpha}{I_y}} = \sqrt{\lambda_1 \cdot \lambda_2} = \omega_{ndat} \tag{15}$$

ζ_{dat}, ω_{nsp} represents the damping factor and the undamped natural frequency corresponding to the full scale UAV and are also the values that we want to obtain for the small scale UAV by modifying the parameters, f_s, p_1 and p_2.

Considering:

$$\begin{aligned}
\frac{M_q}{I_y} &= \frac{\frac{1}{4}\rho u_0 cma^2 SC_{mq}}{I_y} \\
\frac{Z_\alpha}{m_{av}u_0} &= \frac{u_0 \cdot Z_w}{m_{av}u_0} = \frac{\frac{1}{2}\rho u_0 SC_{Z\alpha}}{m_{av}} \\
\frac{M_\alpha}{I_y} &= u_0 \cdot \frac{M_w}{I_y} = \frac{u_0 \frac{1}{2}\rho u_0 cmaSC_{m\alpha}}{I_y} \\
\frac{M_{\dot{\alpha}}}{I_y} &= u_0 M_{\dot{w}} = \frac{u_0 \frac{1}{4}\rho cma^2 SC_{m\dot{\alpha}}}{I_y}
\end{aligned} \tag{16}$$

the following relations (17) we obtained for ζ_{sp} and ω_{nsp} as a function of f_s p_1 and p_2.

$$\omega_{nsp} = \sqrt{\frac{Z_\alpha}{m_{av}u_0}\frac{M_q}{I_y} - \frac{M_\alpha}{I_y}}$$

$$= \sqrt{\frac{\frac{1}{2}\rho u_0 S C_{Z\alpha}}{m_{av}}\frac{\frac{1}{4}\rho u_0 cma^2 S C_{mq}}{I_y} - \frac{u_0\frac{1}{2}\rho u_0 cma S C_{m\alpha}}{I_y}} \qquad (17)$$

$$= \frac{\rho u_0 Scma}{2}\sqrt{\frac{1}{I_y}\left(\frac{C_{Z\alpha}C_{mq}}{2m_{av}} - \frac{2C_{m\alpha}}{\rho Scma}\right)}$$

$$\zeta_{sp} = \frac{\frac{Z_\alpha}{m_{av}u_0} + \frac{M_q}{I_y} + \frac{M_{\dot{\alpha}}}{I_y}}{2\cdot\omega_{nsp}} = \frac{\frac{C_{Z\alpha}}{cma\ m_{av}} + \frac{cma(C_{m\dot{\alpha}} + C_{mq})}{2I_y}}{\sqrt{\frac{1}{I_y}\left(\frac{C_{Z\alpha}C_{mq}}{2m_{av}} - \frac{2C_{m\alpha}}{\rho Scma}\right)}}$$

A quick conclusion is that if p_2 is fixed and the relations between f_s and p_1 complies with relative density similitude criteria ($p_1 = f_s^3$), then the damping factor (ζ_p) does not depend on the plane scale, which represents a first step in the behavior evaluation of the dynamic similitude between the full scale UAV and the scaled model. This fact is represented in the formula (18).

$$\zeta_{sp_2} = \frac{\frac{C_{Z\alpha}}{cma_1 \cdot fs \cdot m_{av_1} \cdot p1} + \frac{cma_1 \cdot fs \cdot (C_{m\dot{\alpha}} + C_{mq})}{2 \cdot I_{y_1} \cdot fs^2 \cdot p1 \cdot p2}}{\sqrt{\frac{1}{I_{y_1} \cdot fs^2 \cdot p1 \cdot p2}\left(\frac{C_{Z\alpha} C_{mq}}{m_{av_1} \cdot p1} - \frac{2C_{m\alpha}}{\rho \cdot S_1 \cdot fs^2 \cdot cma_1 \cdot fs}\right)}} = \frac{\frac{1}{fs^4}\left(\frac{C_{Z\alpha}}{cma_1 \cdot m_{av_1}} + \frac{cma_1 \cdot (C_{m\dot{\alpha}} + C_{mq})}{2 \cdot I_{y_1}}\right)}{\frac{\mathbf{1}}{fs^4}\sqrt{\frac{1}{I_{y_1}}\left(\frac{C_{Z\alpha} C_{mq}}{m_{av_1}} - \frac{2C_{m\alpha}}{\rho \cdot S_1 \cdot cma_1}\right)}} = \zeta_{sp_1} \quad (18)$$

5 Gliding flight tests, comparation with theoretical results

In this case the UAV is performing several gliding flight segments, this evolution was conveniently chosen to be able to extract the parabolic polar approximation, respectively the lift and drag coefficients.

The equations of the gliding flight:

$$\frac{\rho}{2} \cdot S \cdot V^2 \cdot C_Z = G \cdot cos(\gamma)$$
$$\frac{\rho}{2} \cdot S \cdot V^2 \cdot C_X = G \cdot sin(\gamma) \quad (19)$$

Drag polar approximation:

$$C_x = C_x min + \frac{1}{\pi \cdot Ar \cdot e}(C_z - C_z min)^2, Raymer \quad (20)$$

$$C_x = C0 + C1 \cdot C_z + C2 \cdot {C_z}^2, \quad (21)$$
$$second\ degree\ polinomial\ equation$$

The first expression (20) has the advantage that the three coefficients have other meanings: e – Oswald's number, $C_x min$ – minimum value for C_x, $C_z min$ –minimum value for C_z.

In any case, C_x and C_z are replaced and from the parabolic approximation a relation is obtained in which the unknowns are $C_x min$, $C_z min$ and e, respectively C0, C1 and C2.

The other parameters have the following values:

$$G = 42N, S = 0.761m^2, \rho = 1.225 \frac{kg}{m^3} \text{and } Ar = 9.438.$$

$$\frac{G \cdot sin(\gamma)}{\frac{\rho}{2} \cdot S \cdot V^2} = C0 + C1 \cdot \frac{G \cdot cos(\gamma)}{\frac{\rho}{2} \cdot S \cdot V^2} + C2 \cdot \left(\frac{G \cdot cos(\gamma)}{\frac{\rho}{2} \cdot S \cdot V^2} \right)^2 \quad (22)$$

Equation (22) has the unknowns: C0, C1 and C2 (polynomial coefficients)

$$\frac{G \cdot sin(\gamma)}{\frac{\rho}{2} \cdot S \cdot V^2} = C_x min + \frac{1}{\pi \cdot Ar \cdot e} \left(\frac{G \cdot cos(\gamma)}{\frac{\rho}{2} \cdot S \cdot V^2} - C_z min \right)^2 \quad (23)$$

Equation (23) has the unknowns: e (Oswald's number), $C_x min$ and $C_z min$

In any situation we have 3 unknowns which requires solving a 3 equations system. We basically have the same equality from above but used in 3 calculation points: three speed values and three values of the gliding path γ corresponding to the speeds.

From telemetry data, 3 flight segments were extracted using the following criteria:

- straight flight;
- constant speed (constant gliding path) with deviations up to ± 0.5 m/s;
- pitch, roll and yaw angles, are constant or null depending on the reference system;
- the flight segment is long enough so that there is no interference due to the movement history.

Table 5.1. Features of Paths Flight

	Time-frame, $T_{initial} - T_{final}$ [s]	Altitude difference [m]	Flight speed [m/s]	Distance calculated [m]	Distance measured with GPS [m]	Gliding slope [degrees]
Route I	2049,38-2042,77 = 6,61	11.5	25.694	169.84	176	3.883
Route II	2648,21-2626,19 = 22,02	22	18.306	403.088	424	3.129
Route III	2930,43-2894,33 = 36,01	31.8	15.278	551.528	625	3.305

Having three equations (22) or (23) I have obtain the following values for polynomial coefficients and with these coefficients Cx and Cz can be calculated. The values can be found in Table 5.2.

Table 5.2. Polynomial coefficients

C0	0.007139
C1	0.002444
C2	0.095
$C_x min$	0.007123
$C_z min$	-0.013
E	0.353

Table 5.3. Polynomial coefficients

Cz (result from flight logs)		Cx (Result of flight logs)		CZ1/Cx1 (measured)	CZ1/Cx1 (theoretic)
Cz1	0.136	Cx1	0.009241	14.78	18.34
Cz2	0.269	Cx2	0.015	17.93	20.37
Cz3	0.385	Cx3	0.022	17.5	19.05

The resulting polynomial equation with the above coefficients is compared with the XFLR theoretical results. In the graph below we have increased the value of the theoretical Cx with 0.0018 to overlap with the experimental results. We can conclude that flight tests detected a drag increase with 0.0018 and if we consider this to $C_x min$ we can say that we have an increase in the minimum drag by 20 %.

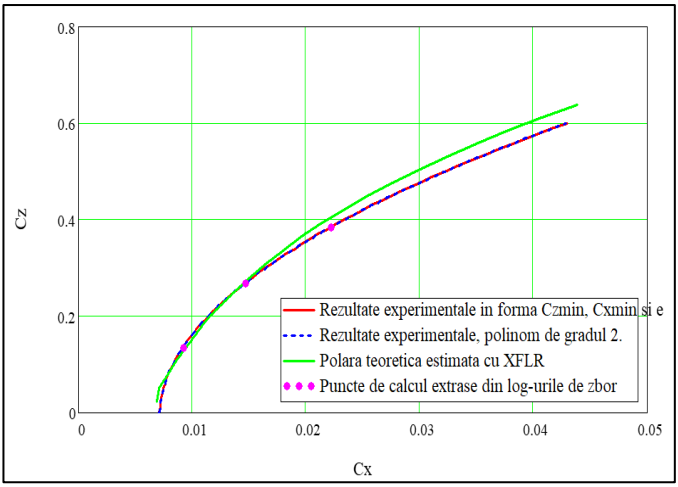

Fig. 5.1. Graphic comparison.

The results differ significantly because of several reasons:

- The polar calculated with XFLR uses the VLM method that involves several other approximations, including the assumption that the angles are small. Also, the geometry of the fuselage is approximated.
- Geometric differences resulting from the manufacturing of the real plane, an important aspect is the thickness of the trailing edge which in theoretical calculations had almost zero thickness.
- Speed and altitude measurement errors.

The method is based on a 2nd degree polynomial equation given by 3 calculation points, the more distanced these points are, the better the results are. Moreover, if we have more calculation points,

we obtain a better approximation. In this case the comparison is valid in the Cz range [0.136; 0.385]. As noted in the graph above, the polar no longer fits outside the range (extrapolated results do not coincide).

6 Estimation of p_1 and p_2 parameters

The purpose of the doctoral thesis is to provide a method of scaling an aircraft in order to obtain a model that is both static and dynamic, such as the real plane in behavior.

A first observation would be that if we keep the same scale factor for gravity center position then certain aerodynamic coefficients remain quasi-constants. This aspect is illustrated in Fig. 6.1. and we can say that the coefficients $CL, CL0, C_L^{\alpha}$, $C_L^{\delta e}, Cm, C_m^{\alpha}, C_m^{\delta e}$ do not change with the scale variation. It also helps that the studied aircraft is a flying wing and the difference in drag resulted from Reynolds variation does not significantly influence the moment coefficient.

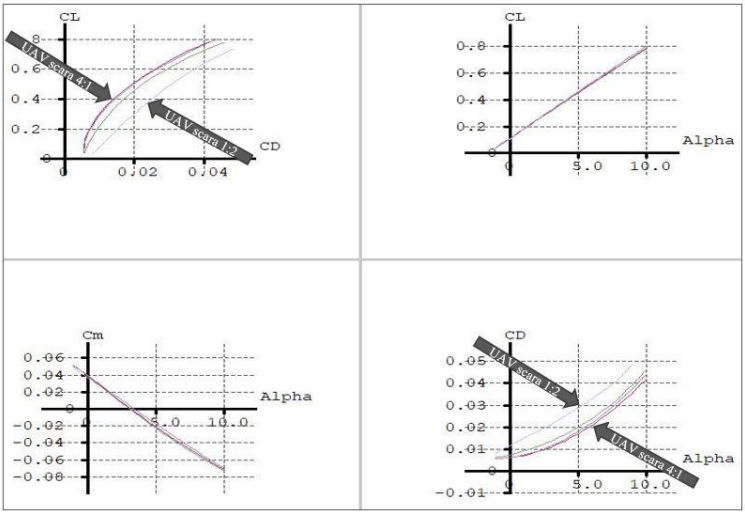

Fig. 6.1. UAV at various scales, horizontal and rectilinear flight, elevator deflection -6 degrees.

The scaling method can be obtained theoretically, using the short period mode approximation where the parameters p_1 and p_2 are obtained for a given value of ζ_{sp} and ω_{nsp}, but also semi-empirical. In the second case the base configuration of UAV Muros is taken as a reference and other versions are generated at other scales (x1.5, x2, x2.5, to x4). The same model previously mentioned is used in order to estimate the aerodynamic performances for the UAVs at other scales, but also p_1 and p_2 of the model airplane.

In Table 6.1 the results are expressed using the theoretical method, where f_s = 1 represents the scale of the model plane for which the mass and inertia moments are multiplied by $p1$ and $p2$.

Table 6.1. Scaling Parameter Values

UAV model ($f_s = 1$)				Real Airplane (scaled)	
p_1	p_2	ω_{nsp}	ζ_{sp}	f_s Real UAV	p_1 for Real UAV ($p_2 = 1$)
1	1	7.08328	0.700643	1	1
1.8831	1.6398	5.7835	0.700643	1.5	3.375
2.7451	2.2524	5.0086	0.700643	2	8
3.6035	2.8585	4.4799	0.700643	2.5	15.625
4.4607	3.4618	4.0895	0.700643	3	27
5.3173	4.0638	3.7862	0.700643	3.5	42.875
6.1737	4.6651	3.5416	0.700643	4	64

From the table above we can say that the real plane built by scaling starting from the model plane has the same damping factor ζ_{sp} and the same natural undamped frequency ω_{nsp}, as the model used in flight tests. An important observation is that the variation of the parameters $p_1$and p_2 with f_s is linear, which means that the method can be extrapolated with very small errors. The calculation method of was made in MATLAB and listed in annex 3.

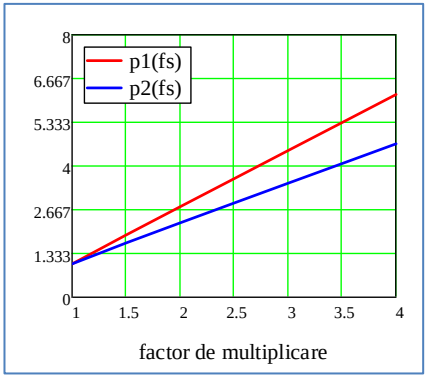

Fig. 6.2. Variation of parameters $p1$ and $p2$ with scale factor – short-period mode

This method has a disadvantage, that it uses only that part of the dynamic system responsible for the short-period mode. A better estimation of these scaling parameters (p_1 and p_2) is obtained if we use the MATLAB programs in annexes 3 and 4. Here we use a function in which we force the equality between the eigenvalues λ, both on the longitudinal and lateral-directional channel (complete matrices 4x4). In particular, the imaginary and real parts of the eigenvalues are equalized, which leads to a system of 8 equations with unknowns p_1 and p_2. The scale factor (f_s) can be set to the desired value. In our case the UAV that can be tested in flight is basically the reference model and is considered at scale 1:1 ($f_s = 1$).

Table 6.2 scaling coefficients, complete matrices

Model plane ($f_s = 1$)				Real Airplane (scaled)	
p_1	p_2	ω_{nsp}	ζ_{sp}	f_s Real airplane	p_1 Real Airplane ()$p_2 = 1$
1	1	7.08328	0,700643	1	1
1.3409	1.4782	5.970743	0,789368	1.5	3.375
1.6633	1.9503	5.268417	0,840095	2	8
1.9986	2.4235	4.769694	0,869236	2.5	15.625
2.3344	2.8959	4.391543	0,888891	3	27
2.6702	3.3679	4.091659	0,903106	3.5	42.875
3.0064	3.8394	3.846285	0,913834	4	64

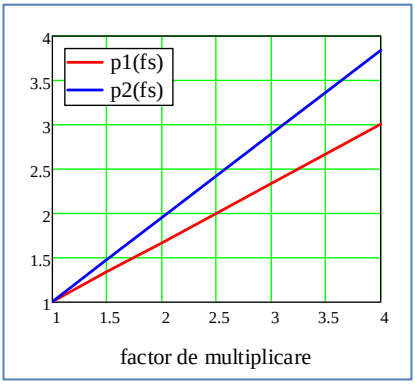

Fig.6.3 Variation of parameters $p1$ and $p2$ with scale factor – Complete matrices

In order to further illustrate the methodology used we will take as an example the multiplication factor 1.5 ($p1 = fs^3 = 3{,}375$, $p2 = 1$), resulting in a real plane with the following specifications:

Table 6.3 Real Airplane Specifications

Properties	Value	U.M.
Airplane mass	$10{,}517 \cdot p1 = 35.5$	kg
Wing surface	$1{,}577 \cdot fs^2 = 3.55$	m^2
Wingspan	$4 \cdot fs = 6$	m
Moment of inertia I_y	$1{,}35 \cdot fs^2 \cdot p1 \cdot p2 = 10{,}25$	$kg \cdot m^2$

For this generated plane resulted in the following own values:

$$\lambda_L = \begin{Bmatrix} -3{,}283056 + 5{,}612509i \\ -3{,}283056 - 5{,}612509i \\ -0{,}020659 + 0{,}615824i \\ -0{,}020659 - 0{,}615824i \end{Bmatrix}, \lambda_{LD}$$

$$= \begin{Bmatrix} -0.068694 + 1.585213\text{i} \\ -0.068694 - 1.585213\text{i} \\ -0.141647 \\ -0.0000148 \end{Bmatrix}$$

For this full-scale aircraft, we have the following specifications for the scaled model, the multiplier coefficients are presented in the previous table.

Table 6.4 Model Plane Specifications

Properties	Value	U.M.
Airplane mass	$10{,}517 \cdot 1{,}3409 = 14{,}1$	kg
Wing surface	$1{,}577$	m^2
Wingspan	4	m
Moment of inertia I_y	$1{,}35 \cdot 1{,}3409 \cdot 1{,}4782 = 2{,}676$	$kg \cdot m^2$

The resulting eigenvalues:

$$\lambda_L = \begin{Bmatrix} -3{,}2596 + 5{,}6153i \\ -3{,}2596 - 5{,}6153i \\ -0{,}0249 + 0{,}6594i \\ -0{,}0249 - 0{,}6594i \end{Bmatrix},$$

$$\lambda_{LD} = \begin{Bmatrix} -0.0584963 + 1.5984166\mathrm{i} \\ -0.0584963 - 1.5984166\mathrm{i} \\ -0.151769 \\ -0.00000929 \end{Bmatrix}$$

The major differences for the eigenvalues between the model and the actual plane are those related to phugoid mode, a percentage difference of not more than 17%. The best approximation is obtained for the short-period mode with differences of less than 1%, which is above the errors and approximations that have gathered along the way.

The above results are considered for the full matrix case. If we examine the short-period mode approximation (theoretical method), the following eigenvalues are obtained:

$$\lambda_L = \begin{Bmatrix} -2{,}707942 + 5{,}494521i \\ -2{,}707942 - 5{,}494521i \\ -0{,}024824 + 0{,}558855i \\ -0{,}024824 - 0{,}558855i \end{Bmatrix},\ \lambda_{LD} =$$

$\begin{Bmatrix} -0.046909 + 1.5199528\mathrm{i} \\ -0.046909 - 1.5199528\mathrm{i} \\ -0.1279866 \\ -0.00000955 \end{Bmatrix}$, where we find that the differences are much larger.

For the previous case I have illustrated in figures Fig. 6.4 - Fig. 6.7 the comparison of the step response between the model plane and the full-scale plane

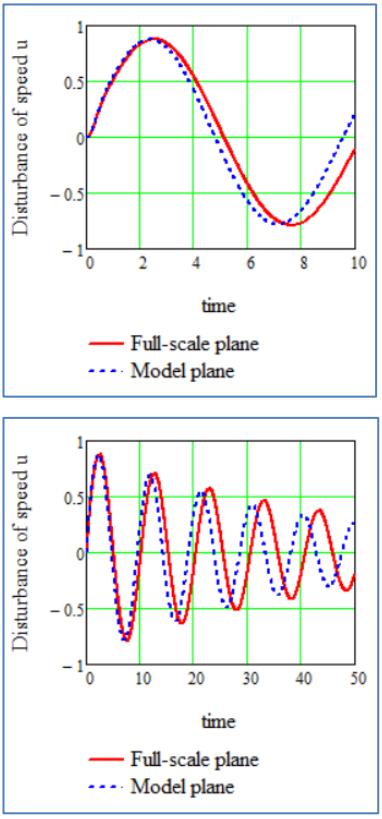

Fig. 6.4. Step Response comparison – u perturbations

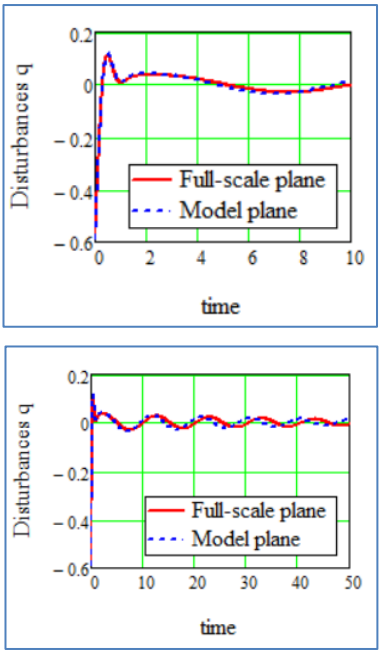

Fig. 6.5 Step Response comparison – q perturbations

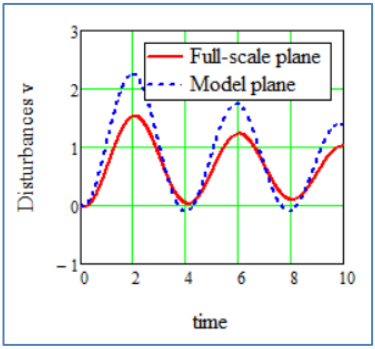

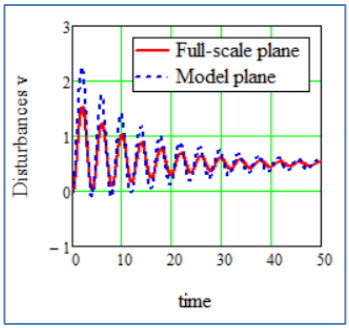

Fig. 6.6 Step Response comparison – perturbations v

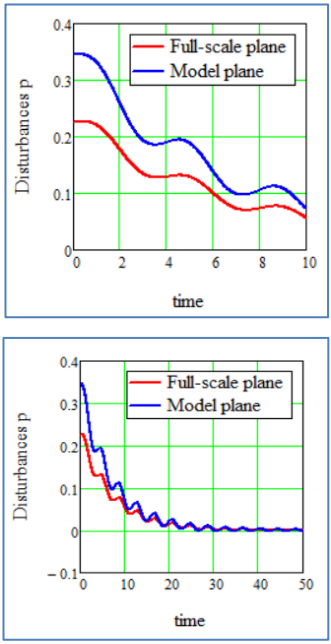

Fig. 6.7 Step Response Comparison – perturbations p

As expected, for perturbations corresponding to the short-period mode (u, q), the results are similar with errors less than 1%. If we refer to the perturbation evolution related to the phugoid mode, then the differences are slightly larger and reach up to 17%. These differences are best illustrated in the example above on the numeric values of the eigenvalues λ, but also in Fig. 6.4 - Fig. 6.7

Both methods were implemented in MATLAB. As input data we have the UAV geometry multiplied by the scale factor at which we add the mass and the moment of inertia weighted by the parameters p_1 and p_2. In addition to the Etkin dynamic model that was implemented we also have the equalities conditions that the MATLAB function " Lsqnonlin " is trying to satisfy. This means that we have not been able to achieve equality but only the best approximation of the terms of equality within the meaning of the smallest squares method thus resulting the output variables p_1 and p_2 for the model plane. What is interesting is that although the solution is an approximate one, for various values of f_s we obtain a linear variation for p_1 and p_2 (Fig.6.3 Linear variation means that the errors are proportionate and the results can be easily extrapolated to other scales.

7 Conclusions and further developments

In the first part is briefly presented the need to generate UAVs at various scales and a way to set up both the geometry and the mass of the UAV in order to generate these new versions. In order to make a quantitative performance assessment, the dynamic model applied to a flying wing UAV was extensively presented, with the assessment of the dynamic model including the system response to a step disturbance, namely elevon deflection.

Scaling method is determined from certain similitude criteria, that is relative density factor. Basically, a relationship is obtained between the scale factor, f_s and the multiplication factor of the mass, p_1. With the above results and in the short-period mode approximation, the analytical method is providing numerical values for $p_1$and p_2 for the scaled model.

A method of testing the scaled models in gliding flight is also presented in order to obtain the plane polar as a polynomial approximation, in our case with a second-degree polynomial relation. This result is very useful because the theoretical results can be compared with the experimental results. In both situations we have errors in calculations or measurements. For the experimental results have a higher degree of uncertainty because certain steps of instruments calibration could not be checked and the flight segment

is represented by just one flight and not an average of several flights that would have been performed under different weather conditions.

In addition to the analytical approach, a semi-empirical estimation of the parameters was also carried out in order to obtain p_1 and p_2. Equality conditions in MATLAB were changed and instead of using the dapping factor respectively the natural undamped frequency related to the short-period mode, we have imposed the equality between imaginary and real parts of the eigenvalues both on the longitudinal and lateral-directional channels, resulting in virtually 8 equality conditions. The results are best highlighted in Chapter 6 example, in which we have generated an UAV at 1.5 scale, and then we have determined the parameters p_1 and p_2 (parameters that multiply the mass and the moment of inertia) of the scaled model. In our case, we considered the model at 1:1 scale. The result is that we have obtained a plane model that has roughly the same dynamic behavior as the real plane. The eigenvalues that correspond to longitudinal channel - short-period mode are approximated with less than 1% differences. For other eigenvalues the differences may reach up to 17%.

The results obtained can be used in the way that the necessary tests can be carried out in flight with the resulting scaled model. If we refer to the example in Chapter 6, we note that if we have a real airplane increased by 1.5 times than the plane model, then the plane model will have a mass multiplied by 1.34 and a moment of inertia

multiplied by 1.48. These values are very easy to implement, in the sense that additional masses can be added to reach the desired value and the same can be achieved with the moments of inertia. In case of inertia moments, the method provides the final value and not the method of distributing the mass inside the model plane in order to obtain these values. With the help of 3D modeling in CATIA or SolidWorks you can easily get the X, Y and Z coordinates of the extra weights that should be added to the plane model. If a scale factor of 1.5 method is feasible, the more scale factor increases, the more flight testing is becoming more restrictive or even impossible for certain configurations.